

# Transactions Briefs

## An Instantaneous and Syllabic Companding Translinear Filter

J. Mulder, W. A. Serdijn, A. C. van der Woerd,  
and A. H. M. van Roermund

**Abstract**—An inherent characteristic of most translinear (TL) filters is *instantaneous* companding. This brief describes a distortionless *syllabic* companding TL filter based on the “analog floating-point technique” [1]. Through the addition of a compensation current to each of the capacitances in the filter, distortion is eliminated. By applying syllabic companding to a TL filter, the input current can be much larger than the quiescent current, thus increasing the dynamic range.

**Index Terms**—Companding, continuous-time filters, current-mode.

### I. INTRODUCTION

A circuit technique receiving increasing interest in the field of analog electronics is the area of translinear (TL) filters. TL filters were introduced by Adams [2] and reintroduced by Seevinck [3]. In both [2] and [3], only first-order filters were presented. The technique was generalized to filters of arbitrary order by Frey [4]. TL filters exploit the exponential law describing the bipolar transistor or the MOS transistor operating in the subthreshold region. A generalization of the underlying principle to the square law behavior of MOS transistors operating in strong inversion was proposed in [5].

TL filters comprise only transistors and capacitors. The superfluity of resistors is an advantage in a low-power environment [6]. Most TL filters are instantaneously companding, which makes them especially interesting for low-voltage designs where the trend to lower supply voltages directly limits the dynamic range obtainable using conventional filter implementation techniques.

The exponential law is exploited not only for companding, but also to implement multiplication of currents using the TL principle [7]. In fact, TL filters can be described completely in terms of currents [8]. As a consequence, they can be regarded as an extension of the TL principle toward dynamic transfer functions. Therefore, we have adopted the term *dynamic translinear principle* [9].

Using the conventional TL principle, it is possible to implement nonlinear static transfer functions. Combining these nonlinear static functions with the dynamic TL principle, it is quite obvious that it will also be possible to apply the dynamic TL principle to the realization of nonlinear dynamic systems. That is, the dynamic TL principle facilitates direct implementation of nonlinear differential equations, e.g., limit cycles (i.e., oscillators) [10], rms-dc conversion [9], and even chaos.

TL filters can also be regarded as a subclass of the class of *distortionless companding* filters. This concept was introduced in [1] and [11] with respect to syllabic companding, where the compression factor is derived from some function of the average strength of the input or output signal. A general description including instantaneous companding—where the compression factor depends on the

Manuscript received June 3, 1996; revised February 28, 1997. This paper was recommended by Associate Editor J. Franca.

The authors are with the Electronics Research Laboratory, Delft University of Technology, 2628 CD Delft, The Netherlands.

Publisher Item Identifier S 1057-7122(98)00992-1.

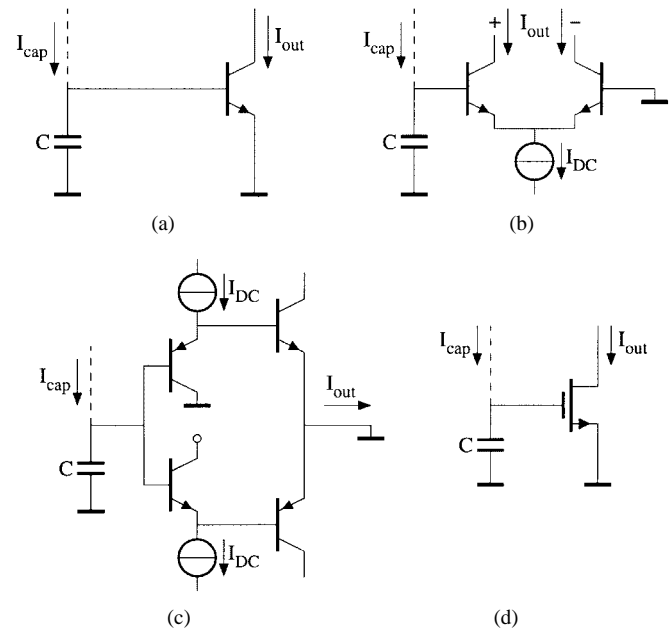


Fig. 1. Generic output structures of (a) log-domain filters, (b) tanh filters, (c) sinh filters, and (d)  $\sqrt{\cdot}$ -domain filters.

instantaneous value of the input or output signal—was presented in [12].

In [11], the distortionless syllabic companding concept was applied to a range-switching  $\Sigma\Delta$  analog-to-digital converter (ADC) and in [1] to a range-switching OTA-C filter. In [13], a continuously-updating operational transconductance-capacitance (OTA-C) filter was reported. In this brief, it is shown that syllabic companding can also be implemented quite elegantly using the dynamic TL principle. Syllabic companding can be applied to increase the dynamic range of a TL filter. First, the instantaneous companding behavior of TL filters is treated in Section II. The theory of distortionless syllabic companding [1], [11]–[13] is explained in Section III and an implementation technique for TL filters is derived. The compensation technique is applied to a TL syllabic companding second-order low-pass Butterworth filter, which is described in Section IV. Simulations, presented in Section V, demonstrate the correct operation of the principle.

### II. INSTANTANEOUS COMPANDING

The class of TL filters can be divided into several subclasses, four of which have been reported in literature. The subclasses of log-domain filters [2], tanh, and sinh filters [14] depend on the exponential behavior of the bipolar transistor, or the MOS transistor in the subthreshold region. The subclass of  $\sqrt{\cdot}$ -domain filters [5] is based on the quadratic behavior of the MOS transistor in the strong inversion region.

In Fig. 1, the generic output structures of these four types of filters are shown. The dynamic TL principle [9] on which all dynamic TL circuits are based can be explained with reference to these output structures. The key to dynamic TL circuits are the capacitance currents, which are nonlinearly related to the collector or drain

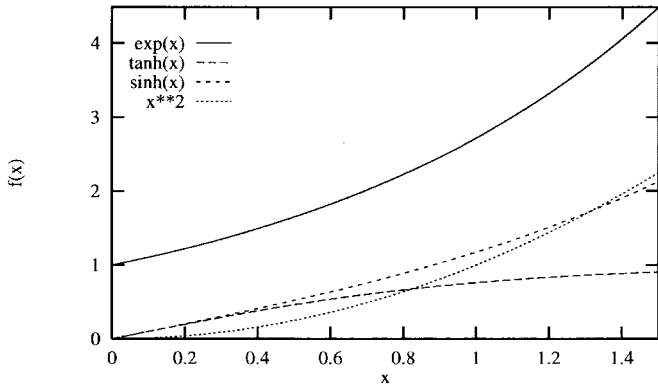


Fig. 2. The  $V - I$  transfer functions of the circuits shown in Fig. 1.

currents. For example, the capacitance current  $I_{cap}$  flowing through the capacitance  $C$  shown in Fig. 1(a), is given by [8]

$$I_{cap} = CU_T \frac{\dot{I}_{out}}{I_{out}} \quad (1)$$

where  $U_T$  is the thermal voltage,  $I_{out}$  is the collector current, and the dot represents differentiation with respect to time. Clearly,  $I_{cap}$  is nonlinearly related to  $I_{out}$ , thus expressing the instantaneous companding inherently present.

The dynamic TL principle becomes clear if we multiply (1) by the strictly positive denominator  $I_{out}$ , which yields

$$CU_T \dot{I}_{out} = I_{cap} \cdot I_{out}. \quad (2)$$

Thus, the dynamic TL principle states that *the derivative of a current can be replaced by a product of currents*. This product of currents is implemented by means of the conventional TL principle [7]. Consequently, the dynamic TL principle can be regarded as a generalization of the conventional, i.e., static TL principle. For tanh, sinh, and  $\sqrt{\cdot}$ -domain filters, similar relations can be found.

Although the voltages in a TL circuit are logarithmically related to the currents, not all TL filters are companding. In Fig. 2, the  $V - I$  transfer functions from the capacitance voltages to the output currents are depicted for the four output structures shown in Fig. 1. Fig. 2 clearly shows that the exponential function, the hyperbolic sine function, and the square function are expanding. In other words, the second derivative of each of these functions is positive for  $x \geq 0$ . However, the hyperbolic tangent function is a compressing function. Therefore, tanh filters are not companding, but show the opposite behavior.

In TL circuits, the instantaneous companding only applies to the  $I - V$  and  $V - I$  conversion at the input and output of the circuit, respectively. Instantaneous companding is interesting with respect to the limited supply voltage. However, this type of companding has very little influence on the currents in a TL filter. The currents are not compressed. It is important to note that instantaneous companding does not affect the input current range of a TL filter. Filters operating in class A, like log-domain,  $\sqrt{\cdot}$ -domain, and tanh filters, need a dc bias current, on which the actual ac input signal is superposed. The maximal amplitude of the input current is restricted to the value of this bias current. Higher values result in clipping distortion.

The dynamic range can be enlarged by class AB operation of the filters. In theory, the dynamic range of class AB TL filters is infinite. However, in practice, the finite current gain of the bipolar transistor limits the maximal current swing to about ten times the value of the quiescent current [15]. Higher values result in soft distortion.

For both class A and class AB TL filters, a further increase of the dynamic range can be accomplished by applying syllabic companding

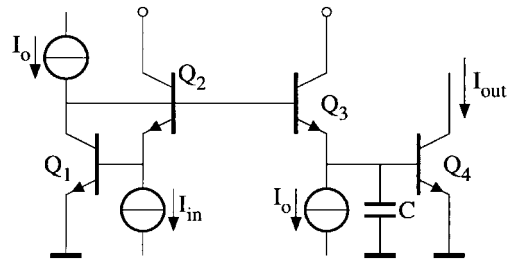


Fig. 3. First-order low-pass TL filter.

based on the analog floating-point technique [1], [11]–[13]. The nature of syllabic companding in TL filters is different from the instantaneous companding inherently present. In a syllabic companding setup, the input current  $I_{in}$  is compressed by multiplying it by a positive signal  $g$ , resulting in a compressed current  $I_{in}^*$ , which is supplied to the core TL filter. When the signal  $g$  is a suitable function of the average strength of  $I_{in}$ , the core TL filter will only have to process relatively small signals, i.e.,  $I_{in}^*$ , irrespective of the amplitude of  $I_{in}$ .

### III. SYLLABIC COMPANDING

The analog floating point technique [1], [11], which theoretically establishes distortionless syllabic companding, will be explained with respect to the TL lossy integrator shown in Fig. 3. This filter is derived from a circuit in [2]. The lossy integrator can be described by a current-mode differential equation [2], [8]:

$$CU_T \dot{I}_{out} + I_{out} I_o = I_{in} I_o. \quad (3)$$

The term  $I_{out} I_o$  on the left-hand side of this equation accounts for the loss of the integrator. This term is realized in the TL circuit through the current source  $I_o$  flowing through transistor  $Q_3$ .

In a syllabic companding system, the input signal is multiplied by a positive factor  $g$  at the input and divided by  $g$  at the output. The value of  $g$  is derived from some measure of the average strength of the input or output signal. In a distortionless companding system, this is equivalent to multiplying the differential equation describing the filter by  $g$  [12], [13]. For the circuit shown in Fig. 3 this yields

$$CU_T g \dot{I}_{out} + g I_{out} I_o = g I_{in} I_o. \quad (4)$$

Since  $g \neq 0$ , (4) still has the same unique solution as (3).

The multiplication and division at the input and output, respectively, can be realized using the TL principle. Since it is not possible electronically to multiply by a dimensionless signal, we transform  $g$  into a current  $I_g$  through the equivalence relation  $g = I_g / I_o$  [16]. The multiplication can now be implemented, e.g., by a TL multiplier [17].

Within the core TL filter only the compressed signals  $I_{in}^*$  and  $I_{out}^*$  are available. Therefore, (4) has to be rewritten in terms of these variables. The relations between the original signals and the compressed ones are described by

$$I_{in}^* = g I_{in} \quad (5)$$

$$I_{out}^* = g I_{out} \quad (6)$$

$$g \dot{I}_{out} = \dot{I}_{out}^* - \frac{\dot{g}}{g} I_{out}^* \quad (7)$$

where (7) is obtained from the time derivative of (6).

Especially note the second term on the right-hand side of (7). This term must be incorporated to ensure distortionless companding. Without this term, significant intermodulation distortion results when the frequency of the compression signal  $g$  is not much lower than the frequency band of the input signal.

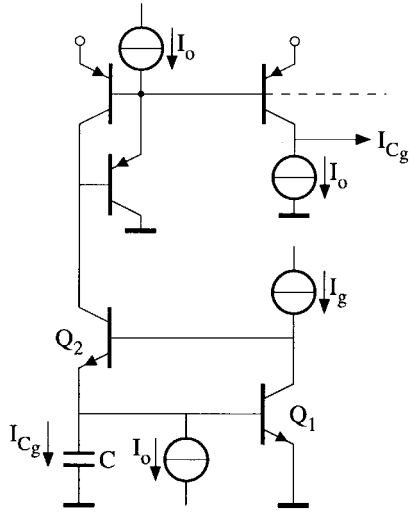


Fig. 4. Generation of the compensation current  $I_{C_g}$ .

Substitution of the above equations in (4) and applying the transformation  $g = I_g/I_o$  yields a differential equation in terms of  $I_{in}^*$  and  $I_{out}^*$ :

$$CU_T \dot{I}_{out}^* + I_{out}^* \left( I_o - CU_T \frac{\dot{I}_g}{I_g} \right) = I_{in}^* I_o. \quad (8)$$

Comparison of this equation with (3) reveals that the compensation term becomes a current  $CU_T \dot{I}_g/I_g$ , which is subtracted from the current  $I_o$  flowing through  $Q_3$  in the lossy integrator shown in Fig. 3. The similarity between this compensation current and the capacitance current described in (1) suggests that the compensation current can be generated by the output structure shown in Fig. 1(a). The circuit of Fig. 4 generates the required compensation current  $I_{C_g}$  from  $I_g$ . The output current  $I_{C_g}$  of this circuit is given by

$$I_{C_g} = CU_T \frac{\dot{I}_g}{I_g}. \quad (9)$$

Substitution of this expression in (8) yields

$$CU_T \dot{I}_{out}^* + I_{out}^* (I_o - I_{C_g}) = I_{in}^* I_o. \quad (10)$$

A current  $I_o$  is added to  $I_{C_g}$  to enable discharging of the capacitance. The compensation current is distributed to the capacitance in the lossy integrator by means of a p-n-p current mirror. As a result, the transfer function of the filter still satisfies the linear differential equation (3).

The form of the compensation term  $\dot{g}/g$  is not specific for TL implementations of syllabic companding [12]. Consequently, the circuit generating this compensation current can be used as an alternative to the implementation presented in [13].

The above description can be generalized to filters of  $n$ th order [12]. The state-space description of an  $n$ th-order filter is multiplied by a time-varying  $n \cdot n$  matrix  $G$ , of which all  $n^2$  elements can in principle be different functions. An implementation of the general principle will result in a considerable overhead. The result will be a fully connected filter topology, requiring  $n^2$  multipliers, dividers, and generators of the different elements of  $G$ . Furthermore, at present, the benefits of such an elaborate implementation over less general implementations are not clear. Therefore, we will restrict ourselves to the situation where one multiplier is placed in front of the core TL filter. This is equivalent to a matrix  $G = g \cdot I$ , where  $g$  is a single compression function and  $I$  the identity matrix of order  $n$ . For TL filters, in this special case, the same compensation current  $I_{C_g}$  has to be distributed to all the capacitances in the  $n$ th-order filter.

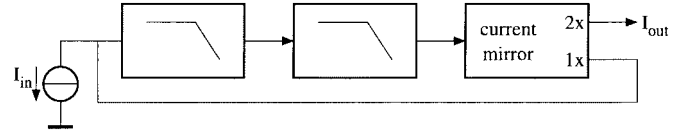


Fig. 5. A second-order low-pass Butterworth filter.

#### IV. A SYLLABIC COMPANDING TRANSLINEAR FILTER

In this section, the analog floating point technique [1], [11] is applied to a second-order low-pass Butterworth filter, applying the compensation circuit developed in the previous section.

A second-order low-pass Butterworth filter can be realized by means of an overall unity negative feedback loop around a cascade of two lossy integrators, resulting in the well-known filter structure shown in Fig. 5. The TL lossy integrator shown in Fig. 3 can be applied in the block schematic shown in Fig. 5. A p-n-p Wilson current mirror inverts the output current of the second lossy integrator before feeding it back to the input. The cutoff frequency  $\omega_c$  of the complete second-order filter is given by  $\omega_c = \sqrt{2}I_o/(CU_T)$ .

In TL filters operating in class A, the actual ac input current  $I_{in}$  is always superposed on a dc bias current  $I_{DC}$ . This bias current limits the maximal input signal level and, hence, the dynamic range of the filter. The dynamic range can be enlarged by compressing  $I_{in}$  before entering the filter. Obviously,  $I_{DC}$  should not be compressed. Otherwise, the input modulation index does not change and, hence, the dynamic range does not improve. Consequently, the compressed current  $I_{in}^*$  should be superposed on the same bias current  $I_{DC}$ .

However, companding introduces local nonlinear behavior. As a consequence, the superposition principle cannot be applied if  $I_{in}$  is compressed, but  $I_{DC}$  is not. If a current  $I_{DC} + I_{in}^*$  is applied to  $Q_2$ , shown in Fig. 3, the compressed output current  $I_{out}^*$  will contain an error term. The relation between  $I_{in}^*$  and  $I_{out}^*$  is described by

$$CU_T \dot{I}_{out}^* + I_{out}^* (I_o - I_{C_g}) - I_{C_g} I_{DC} = I_o I_{in}^*. \quad (11)$$

A comparison of this differential equation with (10) reveals the error: the term  $I_{C_g} I_{DC}$  on the left-hand side of (11).

The error term depends on the compression signal  $g$  and not directly on the input signal  $I_{in}$ . Therefore, in a differential filter setup, which is common practice, the error term is a common mode signal and is eliminated in the differential mode output current. Consequently, we have implemented the filter shown in Fig. 5 in a differential setup.

#### V. SIMULATION RESULTS

The effects of syllabic companding on the differential second-order Butterworth filter were simulated using realistic minimum-sized transistor models from a 3-GHz BiCMOS process. The current gain of the transistors, an important second-order effect in TL circuits, is 180 and 40 for the n-p-n transistors and the vertical p-n-p transistors, respectively.

In Fig. 6, a large-signal (harmonic balance) ac analysis of the filter is shown. In the simulations, the capacitance of the lossy integrator is 1224 pF. The current  $I_o$  is 200  $\mu$ A and  $U_T$  is 26 mV. This results in a cutoff frequency of  $f_c = 1.41$  MHz for the second-order filter.

The dc input current of the Butterworth filter is  $I_{DC} = 400 \mu$ A, resulting in a maximum input current amplitude of 200  $\mu$ A. In the simulation shown in Fig. 6, the modulation index of  $I_{in}$  with respect to the maximal input current amplitude of 200  $\mu$ A is 50%.

Next, the influence of syllabic companding on the distortion of the complete filter was simulated. In theory, a syllabic companding filter has an infinite dynamic range. When  $I_{in}$  has a constant envelope, the signal  $g$  will be constant and the multiplication at the input of the filter

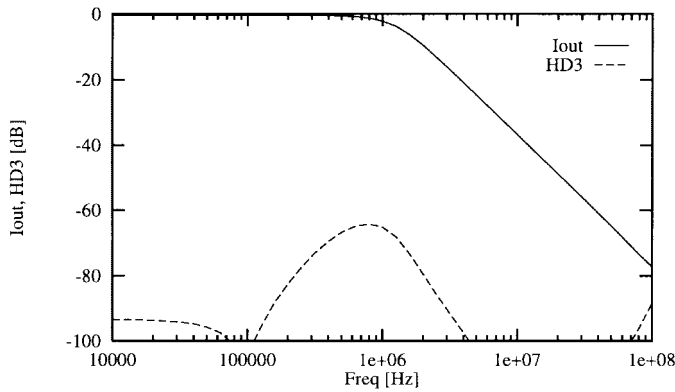


Fig. 6. Large-signal ac analysis of the translinear Butterworth filter without syllabic companding.

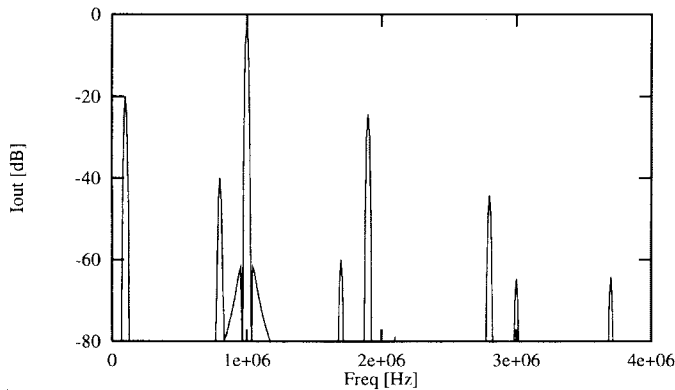


Fig. 7. Output spectrum without compensation for syllabic companding.

does not generate distortion. In a practical syllabic companding setup,  $g$  is generated, e.g., by means of a rectifier followed by a filter [13]. The ripple left on  $g$  for a constant envelope input current, e.g., a sine wave, will determine the distortion of a syllabic companding filter without application of the analog floating-point technique. Therefore, this setup is not very suitable to simulate the effects of the dynamic TL compensation circuit shown in Fig. 4; the results will depend very much on the implementation of the circuit generating the compression signal  $g$ .

Further, the ripple left on  $g$  will contain frequency components at the harmonics of the input current  $I_{in}$ . Consequently, the intermodulation distortion produced by the multiplication of  $g$  and  $I_{in}$  cannot be distinguished from the harmonic distortion of the core TL filter, as these distortion components will be situated at identical frequencies.

As a consequence, for illustration purposes it is much more convenient to define  $g$  independently from  $I_{in}$ .

At low frequencies, with respect to  $\omega_c$ , a time-varying signal  $g$  will not introduce much distortion because the memory of the filter is much shorter than the period of  $g$ . In a worst-case situation, the frequency of  $g$  is close to or above the cutoff frequency of the filter.

In the simulations shown in Figs. 7 and 8,  $I_{in}$  has a frequency of 1 MHz and a modulation index of 50%. The compression signal  $g$ , defined independently from  $I_{in}$ , has a frequency of 900 kHz and a modulation index of 20%, i.e.,  $g = 1 + 0.2 \sin(2\pi \cdot 900 \text{ kHz} \cdot t)$ .

Fig. 7 shows the spectrum of the uncompressed output current  $I_{out}$  without application of the dynamic TL compensation circuit shown in Fig. 4. Clearly, significant intermodulation distortion has resulted from the syllabic companding. The components at the difference and sum frequency are only 20.0 and 24.4 dB, respectively, below the input current level.

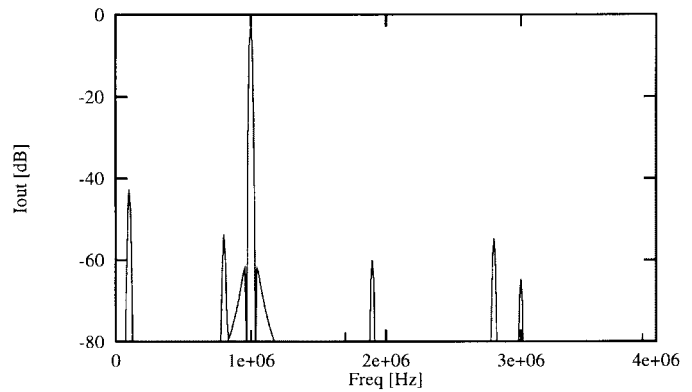


Fig. 8. Output spectrum with compensation for syllabic companding.

In Fig. 8, the compensation circuit is activated, by distributing the current  $I_{C_g}$  to each of the capacitances in the Butterworth filter. The components at the difference and sum frequency are now 42.7 and 60.0 dB, respectively, below the input current level. Consequently, the dynamic TL compensation circuit reduces the distortion by 23 dB. The distortion is not completely eliminated due to second-order effects.

## VI. CONCLUSIONS

In this brief, it was shown that the analog floating-point technique, facilitating distortionless syllabic companding, can be implemented quite easily in TL filters, next to the instantaneous companding inherently present. Distortionless syllabic companding is obtained by generating a compensation current dependent on the compression signal, and adding it to all capacitance currents within the TL. The circuit used to generate the compensation current can also be applied to, e.g., OTA-C filters. The principle was verified through simulations of a second-order translinear Butterworth filter.

## REFERENCES

- [1] E. M. Blumenkrantz, "The analog floating point technique," in *Symp. Low-Power Electron.*, San Jose, CA, 1995, pp. 72–73.
- [2] R. W. Adams, "Filtering in the log domain," presented at the 63rd Conv. A.E.S., New York, LA, May 1979, preprint 1470.
- [3] E. Seevinck, "Companding current-mode integrator: A new circuit principle for continuous-time monolithic filters," *Electron. Lett.*, vol. 26, no. 24, pp. 2046–2047, Nov. 1990.
- [4] D. R. Frey, "Log-domain filtering: An approach to current-mode filtering," *Proc. Inst. Elect. Eng.*, vol. 140, no. 6, pt. G, pp. 406–416, Dec. 1993.
- [5] J. Mulder, A. C. van der Woerd, W. A. Serdijn, and A. H. M. van Roermund, "Current-mode companding  $\sqrt{x}$ -domain integrator," *Electron. Lett.*, vol. 32, no. 3, pp. 198–199, Feb. 1996.
- [6] W. A. Serdijn, A. C. van der Woerd, and A. H. M. van Roermund, "Chain-rule resistance: A new circuit principle for inherently linear ultra-low-power on-chip transconductances or transresistance," *Electron. Lett.*, vol. 32, no. 4, pp. 277–278, Feb. 1996.
- [7] B. Gilbert, "Translinear circuits: A proposed classification," *Electron. Lett.*, vol. 11, no. 1, pp. 14–16, Jan. 1975.
- [8] J. Mulder, A. C. van der Woerd, W. A. Serdijn, and A. H. M. van Roermund, "General current-mode analysis method of translinear filters," *IEEE Trans. Circuits Syst. I*, vol. 44, pp. 193–197, Mar. 1997.
- [9] —, "An RMS-DC converter based on the dynamical translinear principle," in *Proc. European Solid-State Circuit Conf.*, Neuchatel, Switzerland, Sept. 1996, pp. 312–315.
- [10] W. A. Serdijn, J. Mulder, A. C. van der Woerd, and A. H. M. van Roermund, "A wide-tunable translinear second-order oscillator," in *Proc. IEEE ProRISC*, Mierlo, The Netherlands, Nov. 1996, pp. 295–298.
- [11] E. Dijkstra and E. Blumenkrantz, "Low power oversampled A/D converters," in *Proc. Workshop Advances Analog Circuit Design*, Eindhoven, The Netherlands, Mar. 1994.

- [12] Y. Tividis, "General approach to signal processors employing companding," *Electron. Lett.*, vol. 31, no. 18, pp. 1549–1550, Aug. 1995; also vol. 32, no. 9, p. 857, Apr. 1996.
- [13] Y. Tividis and L. Dandan, "Current-mode filters using syllabic companding," in *Proc. ISCAS*, vol. 1, Atlanta, GA, May 1996, pp. 121–124.
- [14] D. R. Frey, "A general class of current mode filters," in *Proc. ISCAS*, vol. 2, Chicago, IL, May 1993, pp. 1435–1438.
- [15] C. C. Enz, "Low-power log-domain continuous-time filters: An introduction, presented at the Low Power–Low Voltage Workshop ESSCIRC '95, Lille, France, Sept. 1995.
- [16] J. Mulder, W. A. Serdijn, A. C. van der Woerd, and A. H. M. van Roermund, "A current-mode synthesis method for translinear companding filters," presented at the ISCAS '97, Cairo, Egypt, Dec. 1996.
- [17] E. Seevinck, *Analysis and Synthesis of Translinear Integrated Circuits*. Amsterdam, The Netherlands: Elsevier, 1988.

## The Study of the Relation Between $R_n - G_n$ Noise Model and $E_n - I_n$ Noise Model of an Amplifier

Jiansheng Xu, Yisong Dai, and Li Yaqen

**Abstract**—The  $R_n - G_n$  noise model can only be used in the case of microwave low-noise amplifier design. Its application scopes are limited and in particular, it cannot be used in low-frequency low-noise amplifier design. This paper has adopted the  $E_n - I_n$  noise model with spectral correlative coefficient (SCC) so that it can be used not only in high-frequency and narrow-band, but also in low frequency, source reactance, and wide-band amplifier low-noise design. In this paper, the equivalent relation between the  $E_n - I_n$  noise model and the  $R_n - G_n$  noise model is derived, and the measurement method of the  $E_n - I_n$  noise model parameters and the measurement results are given. The  $R_n - G_n$  noise model parameters can be accurately obtained by use of the equivalent relation.

**Index Terms**—Amplifiers, noise model equivalence, spectral correlative coefficient.

### I. INTRODUCTION

In microwave-band low-noise amplifier design, the noise performance of an amplifier can be represented by  $R_n - G_n$  noise model parameters, namely the equivalent noise resistance  $R_n$ , equivalent noise conductance  $G_n$ , and the correlation admittance  $Y_{\text{cor}} = G_{\text{cor}} - jB_{\text{cor}}$ . The  $R_n - G_n$  noise model can still be used to calculate amplifier low-noise design parameter  $F_0$ ,  $G_0$ , and  $B_0$ , in which  $F_0$  is the minimum noise figure which occurs for an optimum source admittance whose real and imaginary parts are, respectively,  $G_0$  and  $B_0$ . In terms of  $G_0$ ,  $B_0$ , and  $F_0$ , the noise figure of an amplifier becomes

$$F = F_0 + \frac{R_n}{G_s} \left[ (G_s - G_0)^2 + (B_s - B_0)^2 \right] \quad (1)$$

Manuscript received February 6, 1996; revised March 31, 1997. This work was supported by the China National Natural Science Foundation under Contract 69672023. This paper was recommended by Associate Editor J. Franca.

The authors are with the Department of Electronic Engineering, Jilin University of Technology, Changchun, 130025 China.

Publisher Item Identifier S 1057-7122(98)00970-2.

where

$$F_0 = 1 + 2R_n(G_{\text{cor}} + G_0)$$

$$G_0 = \sqrt{\frac{G_n + R_n G_{\text{cor}}^2}{R_n}}$$

$$B_0 = -B_{\text{cor}}$$

Although the  $R_n - G_n$  noise model has been widely used in microwave-amplifier low-noise design, there still exist some defects. The  $R_n - G_n$  noise model is usually obtained through the measurement of the noise figure. However, the noise figure cannot be measured directly in low-frequency band. Therefore, its application scopes have some limitations, especially if the source impedance is pure reactance, namely  $G_s = 0$ , where the noise figure concept cannot be applied because of  $F = \infty$ . Also, for wide-band amplifier low-noise design, the model has the some difficulties. Thus, the  $R_n - G_n$  noise model can only be used in the cases of microwave-band, narrow-band, and source-impedance ( $G_s \neq 0$ ) amplifier low-noise design. However, with the development of infrared detector, acoustics, and transducer technology there is an urgent need for low-frequency and wide-band amplifier low-noise design. Therefore, we have to use other models to solve these problems.

The  $E_n - I_n$  noise model was first proposed by Rothe and Dahlke [1], [2] in 1956, and was then systematized by Motchenbacher and Fitchen. Its advantages are that the model can be used in low-frequency wide-band amplifier low-noise design through the calculation of equivalent input noise power  $E_{n_s}^2$ . The problem is that the model has the correlation coefficient  $C$ , which allows the model to only be used in source resistance. The model is also not equivalent to the  $R_n - G_n$  noise model.

According to the  $E_n - I_n$  noise model, we have considered the spectral correlative coefficient (SCC)  $\gamma$  in this paper, with the goal of making the model perfect. The improved  $E_n - I_n$  noise model has a definite physics concept, can be used in microwave and low-frequency bands, and can also be used in the conditions of source reactance and wide band. Then, the equivalent relation between the  $E_n - I_n$  noise model and the  $R_n - G_n$  noise model has been derived, which proves that the  $E_n - I_n$  noise model with SCC ( $\gamma$ ) is equivalent to the  $R_n - G_n$  noise model, and also shows that the noise model with SCC is reasonably robust. We then discuss the measurement method of the  $E_n - I_n$  noise model parameters. Through the two-model equivalent relation,  $R_n - G_n$  noise model parameters can be accurately obtained by using the  $E_n - I_n$  noise model parameters measured, which means that a new method to measuring  $R_n - G_n$  noise model parameters has been developed.

### II. $E_n - I_n$ NOISE MODEL AND AMPLIFIER NOISE PERFORMANCE EXPRESSION

Let  $e$  and  $i$  denote, respectively, an amplifier equivalent-input random voltage noise and current noise. Their noise power spectral densities are represented by  $S_e(f)$  and  $S_i(f)$ . If they are expressed by a unit band (1 Hz), then  $E_n^2 = S_e(f)$  and  $I_n^2 = S_i(f)$ . The definition of the spectral correlation coefficient of  $e$  and  $i$  noise power is expressed as follows:

$$\gamma = \gamma_1 + j\gamma_2 = \frac{S_{ei}(f)}{\sqrt{S_e(f)S_i(f)}} \quad (2)$$

where  $S_{ei}(f)$  is the cross-spectral density between  $e$  and  $i$ .

It must be noted that the definitions of  $E_n$ ,  $I_n$ , and  $\gamma$  here are completely different from those of  $E_n$ ,  $I_n$ , and  $C$  in [3]. The former